AGU PUBLICATIONS

JGR

Journal of Geophysical Research: Oceans

RESEARCH ARTICLE

10.1002/2017JC013375

Changes in Bottom Water Physical Properties Above the Mid-Atlantic Ridge Flank in the Brazil Basin

Jian Zhao[1,2] and Andreas M. Thurnherr[1]

[1]Lamont-Doherty Earth Observatory, Columbia University, Palisades, NY, USA, [2]Now at Department of Physical Oceanography, Woods Hole Oceanographic Institution, Woods Hole, MA, USA

Key Points:
- Significant long-term changes of deep water properties are identified in and above deep fracture zone canyons in the eastern Brazil Basin
- Between 1989 and 2014, the isopycnals in the bottom water moved downward whereas a small upward trend occurred in the overlying deep water
- The mean vertical divergence in density has reduced the stratification by about 20% in a 500-m-thick deep layer in the eastern Brazil Basin

Correspondence to:
J. Zhao,
jzhao@whoi.edu

Citation:
Zhao, J., & Thurnherr, A. M. (2018). Changes in bottom water physical properties above the mid-Atlantic ridge flank in the Brazil Basin. *Journal of Geophysical Research: Oceans*, *123*, 708–719. https://doi.org/10.1002/2017JC013375

Received 18 AUG 2017
Accepted 12 DEC 2017
Accepted article online 14 DEC 2017
Published online 30 JAN 2018

Abstract Warming of abyssal waters in recent decades has been widely documented around the global ocean. Here repeat hydrographic data collected in 1997 and 2014 near a deep fracture zone canyon in the eastern Brazil Basin are used to quantify the long-term change. Significant changes are found in the Antarctic Bottom Water (AABW) within the canyon. The AABW in 2014 was warmer (0.08 ± 0.06°C), saltier (0.01 ± 0.005), and less dense (0.005 ± 0.004 kg m^{-3}) than in 1997. In contrast, the change in the North Atlantic Deep Water has complicated spatial structure and is almost indistinguishable from zero at 95% confidence. The resulting divergence in vertical displacement of the isopycnals modifies the local density stratification. At its peak, the local squared buoyancy frequency (N^2) near the canyon is reduced by about 20% from 1997 to 2014. Similar reduction is found in the basinwide averaged profiles over the Mid-Atlantic Ridge flank along 25°W in years 1989, 2005, and 2014. The observed changes in density stratification have important implications for internal tide generation and dissipation.

1. Introduction

The Brazil Basin is a deep basin in the western south Atlantic bounded by the continental rise in the west and the Mid-Atlantic Ridge (MAR) in the east. The deep and abyssal water masses are the North Atlantic Deep Water (NADW) and the Antarctic Bottom Water (AABW). These large-scale water masses, formed in the high latitudes of the North Atlantic and the Southern Ocean, not only ventilate the deep basins but also set up the vertical density stratification of the abyssal ocean. The AABW enters the Brazil Basin mostly through two gaps that intersect the Rio Grande Rise: the Vema Channel (nominal depth ~4,600 m) and the Hunter Channel (~4,200 m) (Figure 1; Hogg et al., 1982; Speer & Zenk, 1993; Zenk et al., 1999). The AABW in both channels is located below 3,000 m, with about 4 Sv transported through the Vema Channel and 2.9 Sv through the Hunter Channel (Hogg et al., 1999; Zenk et al., 1999). Overlying the AABW is the NADW, which is formed in the Greenland-Iceland-Norwegian Seas and in the Labrador Sea. The NADW is transported into the South Atlantic predominantly in the deep western boundary current (DWBC) attached to the Brazilian continental slope. It then splits into two distinct pathways: one continues as a DWBC and the other feeds broad eastward zonal flows across the interior ocean (Hogg & Owens, 1999; Hogg & Thurnherr, 2005; Speer et al., 1995; Talley & Johnson, 1994; Thurnherr & Speer, 2004). The NADW-AABW interface is delineated by the 1.8°C–2°C isotherms, corresponding to the potential (σ_4) range of 45.82–45.90 kg m^{-3} (Hogg et al., 1982; Whitehead & Worthington, 1982).

The AABW is converted to lesser densities by downward diffusion of heat via turbulent mixing processes (e.g., Munk, 1966). In the 1990s, the Brazil Basin Tracer Release Experiment (BBTRE) found intense turbulent diapycnal mixing near the fracture zones (FZs) on the western flank of the MAR (Ledwell et al., 2000; Polzin et al., 1997; L. St. Laurent et al., 2001; L. C. St. Laurent et al., 2001). Tidally forced breaking internal waves were proposed as the primary physical mechanism for the elevated mixing (Nikurashin & Legg, 2011; Polzin et al., 1997). However, Thurnherr et al. (2005) point out that most of the diapycnal buoyancy fluxes inferred from the microstructure data occur inside the 500–1,000 m deep ridge-flank FZ canyon rather than above the topographic envelope. In addition, current meters deployed for 2 years within the FZ revealed that the velocity inside the canyon not only has semidiurnal and diurnal tidal motions but also shows dramatic inertial and subinertial flows (Thurnherr et al., 2005; Toole, 2007). The subinertial motions are enhanced within the canyon and reach magnitudes of several cm/s, similar to the barotropic tidal currents. Thurnherr et al. (2005) argue that hydraulic processes associated with the subinertial along-canyon flow passing across sills

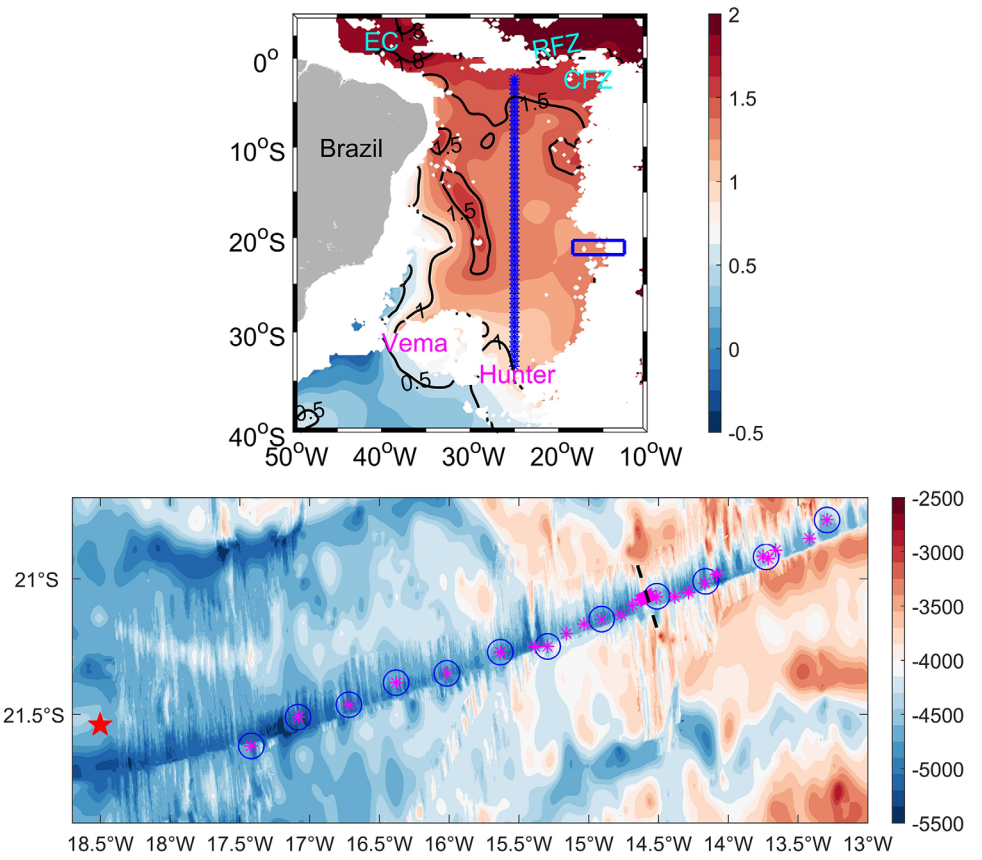

Figure 1. (top) Annual mean potential temperature at 4,000 m (°C) from World Ocean Atlas 2013 is shown in color and with labeled black contours. The locations of the Vema and Hunter Channels are marked. The bottom waters exit the Brazil Basin through the RFZ (Romanche Fracture Zone), CFZ (Chain Fracture Zone), and EC (Equatorial Channel).The hydrographic stations from the WOCE A16S section are shown as blue crosses. The blue box shows the FZ canyon in this study. (bottom) Combined multibeam/satellite topography near the FZ canyon studied during BBTRE and here (color, m), as well as the hydrographic stations used in the data analysis. Blue circles denote stations occupied in 1997. The data collected in 2014 (magenta asterisks) include tow-yo profiles near a prominent sill (black dashed line near 14.6°W). Red pentagram indicates the location of six repeat HRP profiles collected in 1996.

on the canyon floor contribute significantly to the elevated diapycnal mixing in the canyon. This inference has recently been confirmed by data from the Dynamics of Mid-Ocean Ridge Experiment (DoMORE) project (Clément et al., 2017).

Abyssal warming trends in the South Atlantic Ocean have been widely described, especially in the Scotia Sea, the Argentine Basin, and the Brazil Basin (Coles et al., 1996; Johnson & Doney, 2006; Johnson et al., 2014; Kouketsu et al., 2011; Purkey & Johnson, 2010). The northward flowing AABW in the Vema Channel has been found to maintain a general decadal warming trend since the early 1990s (Zenk & Hogg, 1996; Zenk & Morozov, 2007; Zenk & Visbeck, 2013). This is in agreement with the overall AABW warming signal across the whole Brazil Basin documented by repeat hydrographic surveys (Desbruyères et al., 2016; Herrford et al., 2017; Johnson & Doney, 2006; Johnson et al., 2014). In addition, the AABW shows a contraction in the Southern Ocean and along its northward path into the South Atlantic Ocean. The contraction is characterized by descending isotherms (Purkey & Johnson, 2012). On the other hand, although a weak cooling in the lower NADW has been identified in the Equatorial Channel, the NADW in the south Atlantic has not shown any significant decadal changes until now (Herrford et al., 2017; Johnson et al., 2014).

While the abyssal waters are being continuously modified by diapycnal mixing, it remains unclear how the observed long-term changes in the large-scale water masses affect the local hydrography near the rough bathymetry where elevated diapycnal mixing is observed. Changes in the large-scale water masses can alter the local vertical density stratification, which affects internal wave generation, propagation and breaking. In

addition, a heat budget calculation in the Brazil Basin suggests that even a small increase in mixing rates can produce a basin-wide deep warming (Purkey & Johnson, 2012). This study compares hydrographic data collected during BBTRE in 1997 and as part of DoMORE in 2014 with the aim to assess the decadal hydrographic changes over the rough topography of the MAR flank in the Brazil Basin, and to discuss their potential influences on the mixing rates near the FZs.

2. Data and Methods

The study region is a deep FZ canyon on the western flank of the MAR near 21°S (Figure 1). The canyon intersects the ridge flank and extends from the bottom of the Brazil Basin below 5,500 m near 26°W to the MAR crest near 12°W, where the connection to the eastern basin is blocked below 3,000 m. An important bathymetric feature in the FZ canyon is a prominent sill/constriction near 14.6°W where Thurnherr et al. (2005) and Clément et al. (2017) found the largest horizontal near-bottom along-canyon density gradient and the strongest diapycnal mixing. Two hydrographic surveys were carried out with stations along the canyon in 1997 and 2014 during the BBTRE and DoMORE projects, respectively. During the DoMORE survey, tow-yo hydrographic casts were performed near the sill to further define the cross-sill hydrographic structure. A total of 34 conductivity-temperature-depth (CTD) profiles were selected from the DoMORE data to construct an along-canyon section. This section includes 12 stations from the BBTRE survey that were reoccupied during DoMORE with the aim to quantify decadal changes in the canyon hydrography (Figure 1). All sensors of the SBE 9plus CTD from both BBTRE and DoMORE were precruise calibrated, and there are no indications for significant drifts in any of the data. The salinity data are reported in the Practical Salinity Scale 1978 (PSS-78). During the DoMORE cruise, conductivity sensor performance was monitored by a Guildline Portasal SA10 using IAPSO standard seawater (SSW) from batch 149. The analysis of differences between calibrated CTD salinity and sampled water salinity suggests an uncertainty of 0.001 with reference to the IAPSO SSW. We note, however, that batch-to-batch differences for IAPSO SSW can be as large as 0.002 (PSS-78) (Kawano et al., 2006). Overall, the temperature and salinity uncertainties for the data used in this study are estimated to be about 0.001°C–0.002°C and 0.002, respectively.

The 12 repeat CTD station-pairs are used to compute the hydrographic changes between 1997 and 2014. The postprocessed hydrographic profiles are vertically smoothed with a Hanning filter with a 20 dbar half-width and linearly interpolated to a 10 dbar pressure grid. For each profile pair, temperature, salinity, and density coordinate grids are generated with grid steps of 0.005°C, 0.004, and 0.002 kg m^{-3}, respectively. To generate the temperature, salinity, and density grids, data within 200 m of the bottom are disregarded because the stratification at this depth tends to be very weak, causing nonmonotonicity in the density, temperature, and salinity profiles. The bottom waters were kept for the analysis in depth space. The short-term temporal variability of the hydrography in the canyon is inferred from a high-resolution profiler (HRP) repeat station occupied in 1996 (Figure 1). The six repeat HRP profiles were collected within 2 weeks (Polzin et al., 1997). The HRP temperature and pressure sensors were calibrated before and after the sampling cruise and the salinities were adjusted by fitting the deep temperature-salinity (θ–S) properties to profiles from nearby CTD stations occupied during the same cruise (Thurnherr & Speer, 2003).

In addition, the long-term changes in the Brazil Basin are estimated from a repeat hydrographic section along 25°W. It was occupied in 1989, 2005, and 2014 first in the context of the World Ocean Circulation Experiment (WOCE) and more recently as part of the international Global Ocean Ship-based Hydrographic Investigations Program. The section is named A16S, and Johnson et al. (2014) provide more details about the three surveys. The overall measurement accuracies are about 0.001°C–0.002°C for temperature, 0.002 for salinity, and 3 dbar for pressure. All available stations within the latitude range between 2°S and 32°S are utilized to represent the hydrography in the Brazil Basin during each survey period.

Since there are only 12 station pairs from the FZ canyon available, the statistical evaluation for the comparisons between the 1997 and 2014 properties is performed with a bootstrap method (Hastie et al., 2009). The bootstrap technique can generate many more artificial bootstrap samples, which are used to estimate the statistical accuracy without assuming the underlying distribution. Given that the hydrographic profiles are correlated in the horizontal direction, our data are resampled in moving blocks rather than as single elements (Wilks, 1997). The block length is determined from the horizontal decorrelation scale, which is twice the maximum of the integral of lagged autocovariance in the horizontal direction. The zonal decorrelation

length scales near the FZ canyon vary between 80 and 240 km for the water depths below 2,000 m. The meridional decorrelation length scale for the profiles at A16S is set to 163 km, which is the same with Purkey and Johnson (2010). Different sample sizes, between 100 and 10,000, were tested, resulting in similar error for sample sizes larger than about 1,000. The 95% confidence interval is obtained from the values at the fifth and fifth-last percentiles. As an alternative method, we also estimate the statistical uncertainties with the Student's *t* test, which was used by Johnson et al. (2008) and Purkey and Johnson (2010). All results that are significant at the 95% confidence level in the bootstrap method also pass the Student's *t* test. The results below are based on the bootstrap method.

3. Results

3.1. Hydrographic Structure Near the Canyon

The FZ canyon is filled primarily with AABW (Figure 2). The lateral walls bounding the canyon are defined here as the locations of maximum cross-canyon steepness. These walls have nominal depths of 4,000 m west and 3,300 m east of the sill (14.6°W). The AABW's upper boundary is located above the canyon west of

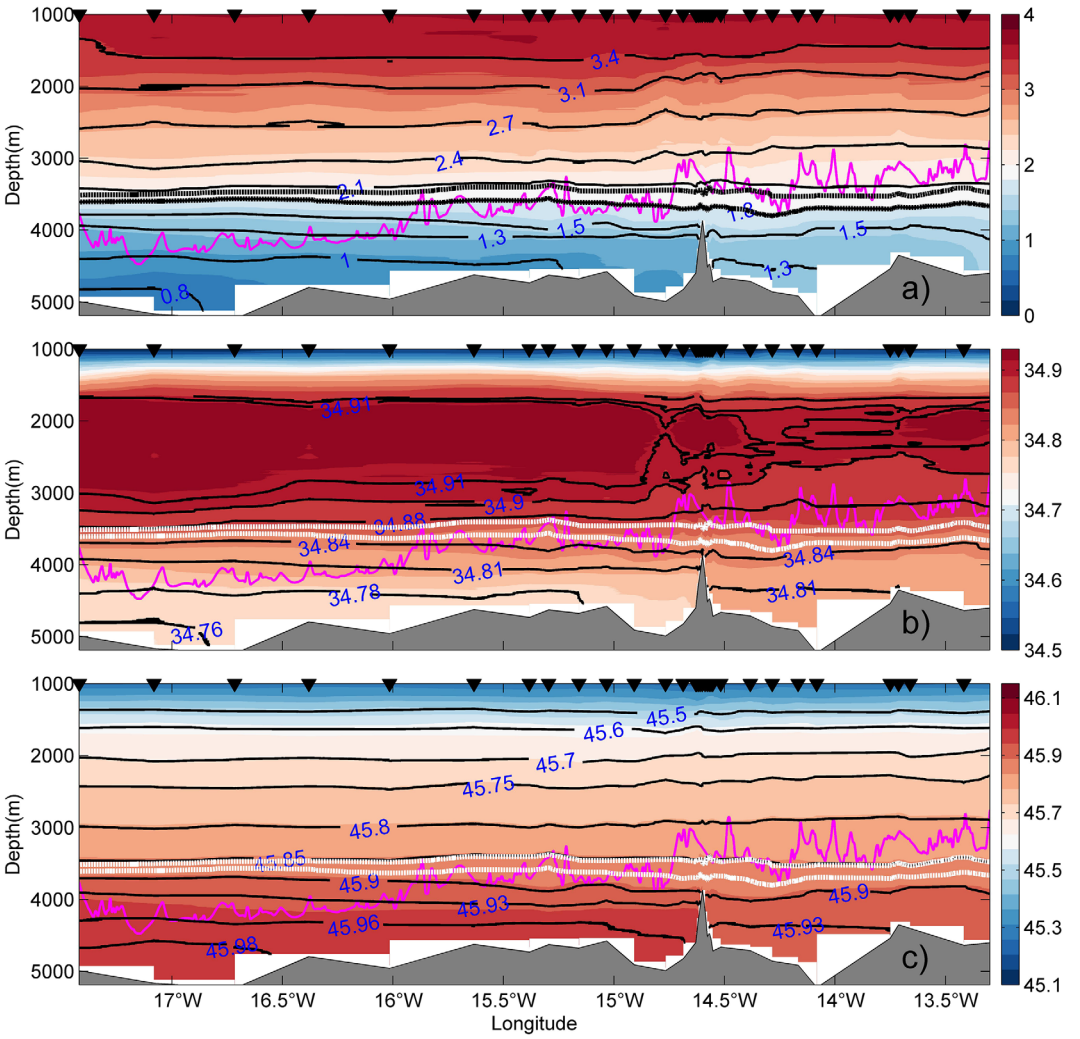

Figure 2. Hydrographic properties along the canyon, using the 2014 DoMORE data. (a) Potential temperature (°C); (b) salinity; (c) σ_4 (kg m^{-3}). The magenta lines define the lateral walls of the canyon. A prominent sill is located near 14.6°W where tow-yo profiles were collected in 2014. The white and black dashed lines mark the 1.8°C and 2°C isotherms, indicating the interface of AABW and NADW. Black triangles mark the locations of the hydrographic profiles in longitude. The bottom bathymetry is from the multibeam data. Each profile reached about 50–100 m above the seabed and the unsampled regions are masked by white.

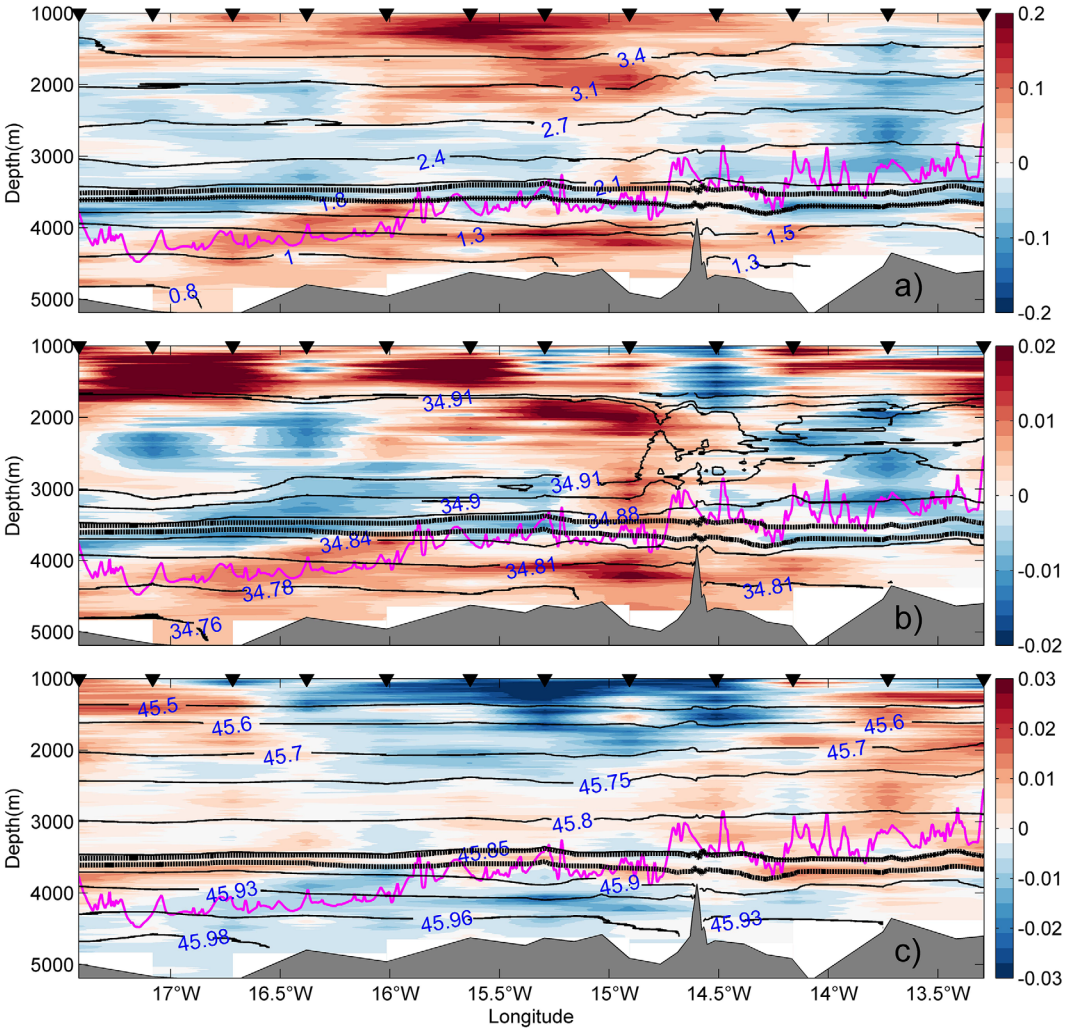

Figure 3. Along-canyon sections of hydrographic differences of (a) Potential temperature (°C); (b) salinity; (c) σ_4 (kg m^{-3}) between 1997 and 2014 (i.e., 2014 minus 1997) shown in color. The black contours show the hydrographic properties in 2014. The magenta lines define the lateral walls of the canyon. The black dashed lines show the 1.8°C and 2°C isotherms, indicating the interface between AABW and NADW in 2014. Black triangles mark the locations of the hydrographic profiles in longitude. The bottom mask is the same as in Figure 2.

16°W and roughly at the depth to the lateral canyon-wall crest east of that longitude. Thus, the canyon in our study region is almost completely filled with AABW. The overlying NADW is characterized by fairly homogenous salinity structure in its core centered around 2,500 m. The salinity in the NADW layer is more uniform west of about 15°W where a high-salinity tongue emanating from the DWBC and carried eastward by mean zonal flow terminates (Thurnherr & Speer, 2004).

Within the canyon, the most striking spatial pattern in the hydrography are the zonal gradients across the sill near 14.6°W, with water masses west of the sill generally colder, fresher, and denser than in the east. The mean abyssal flow within the canyon in the 1990s was found to be eastward based on moored current meters at 17.5°W (Thurnherr et al., 2005; Toole, 2007). More recent observations recorded by current meters and McLane Moored Profilers deployed at the sill near 14.6°W and at 13.7°W also show eastward flow below 3,900 m in 2014/2015 (Clément et al., 2017). The available data thus confirm persistent eastward flow within the canyon, which is essential to maintain a quasi-steady state in the presence of strong diapycnal mixing (L. C. St. Laurent et al., 2001). Through the eastward flow down the mean along-canyon density gradient, the water mass west of the sill is connected with the AABW in the interior of deep Brazil Basin. However, the zonal distribution of the hydrographic properties suggests that AABW is significantly modified when

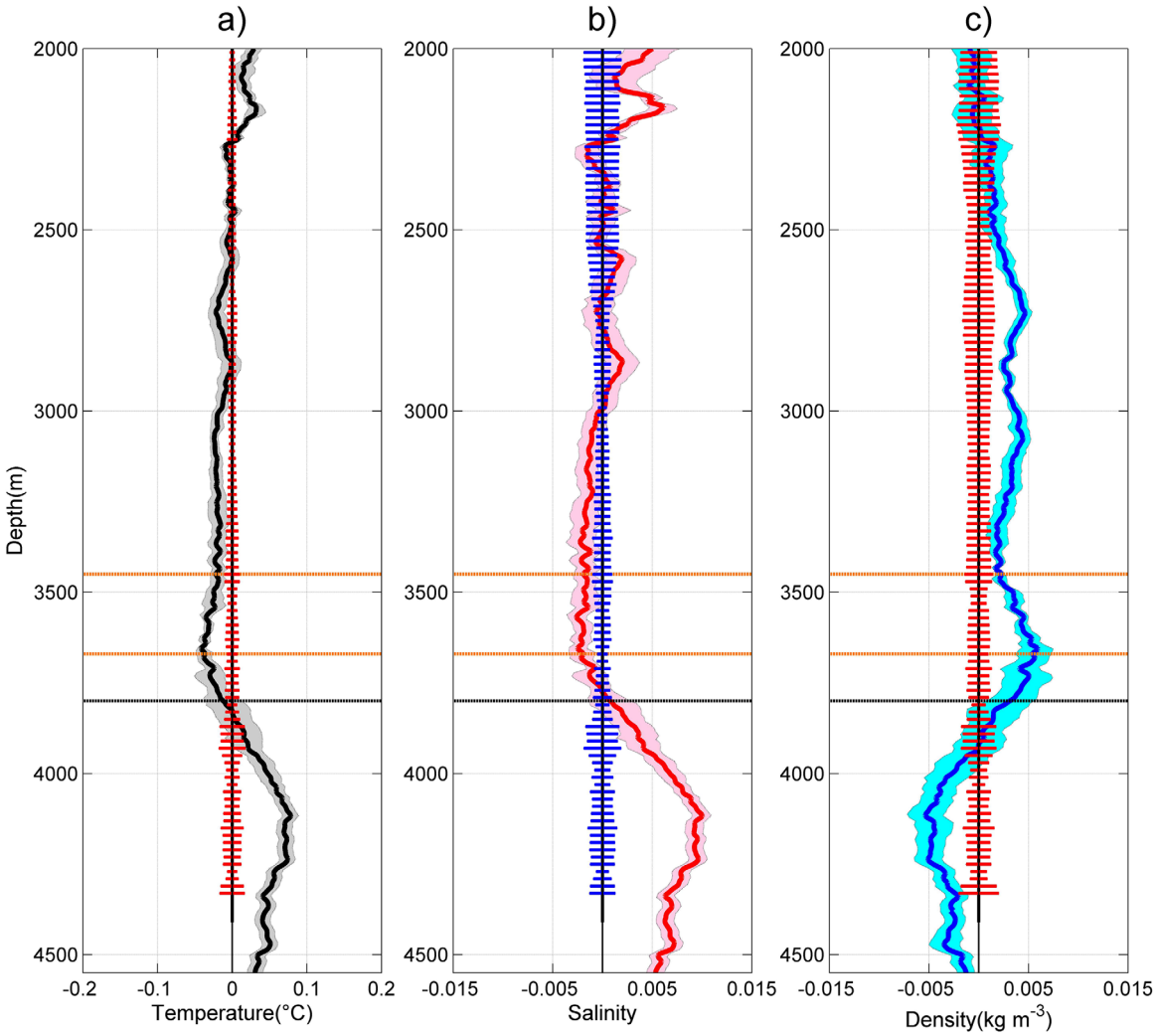

Figure 4. Mean hydrographic differences between 1997 and 2014 (i.e., 2014 minus1997) are shown in (a) Potential temperature; (b) salinity; (c) σ_4. The shaded areas show the 95% confidential intervals estimated using a bootstrap method. The horizontal bars around zero (red and blue) represent the uncertainties associated with high-frequency variability (periods less than 2 weeks), estimated from the six repeat HRP profiles. The orange lines denote the depth levels of the 1.8°C and 2°C isotherms in 2014, and the black lines illustrate the nominal depth of the lateral canyon walls.

passing over the sill. In particular, the densest AABW is warmed by about 0.2°C across the sill, leading to a drop in density (σ_4) of 0.02 kg m^{-3}. This is consistent with Thurnherr et al. (2005) who found that the largest horizontal near-bottom density gradient exists between the hydrographic stations west and east of this sill.

3.2. Hydrographic Change Near the Canyon

The temperature (θ)-salinity curves constructed from the data in 1997 and 2014 indicate that their slopes in the AABW layer are indistinguishable within the measurement uncertainty (dominated by the 0.002 salinity uncertainty). Toole (2007) also noted that the temperature (θ)-salinity relationship at potential temperature below 2.25°C (approximately 3,300 m depth) were stable over the entire BBTRE period (from year 1996 to 2000). The hydrographic changes between 1997 and 2014 are inferred by subtracting the BBTRE from DoMORE data. The differences in the AABW below the lateral canyon-wall crests exhibit approximately uniform structure except at the easternmost two stations (Figure 3). The AABW in 2014 was generally warmer and saltier than in 1997. The mean profiles of temperature and salinity differences calculated from the 12 repeat-station pairs is distinguishable from zero at 95% confidence with mean values that peak at 0.08 $\pm$ 0.03°C and 0.01 $\pm$ 0.003, respectively, over the depth range of 4,100–4,300 m (Figure 4). The density, incorporating both temperature and salinity signals, indicates that the AABW in 2014 at the same depths

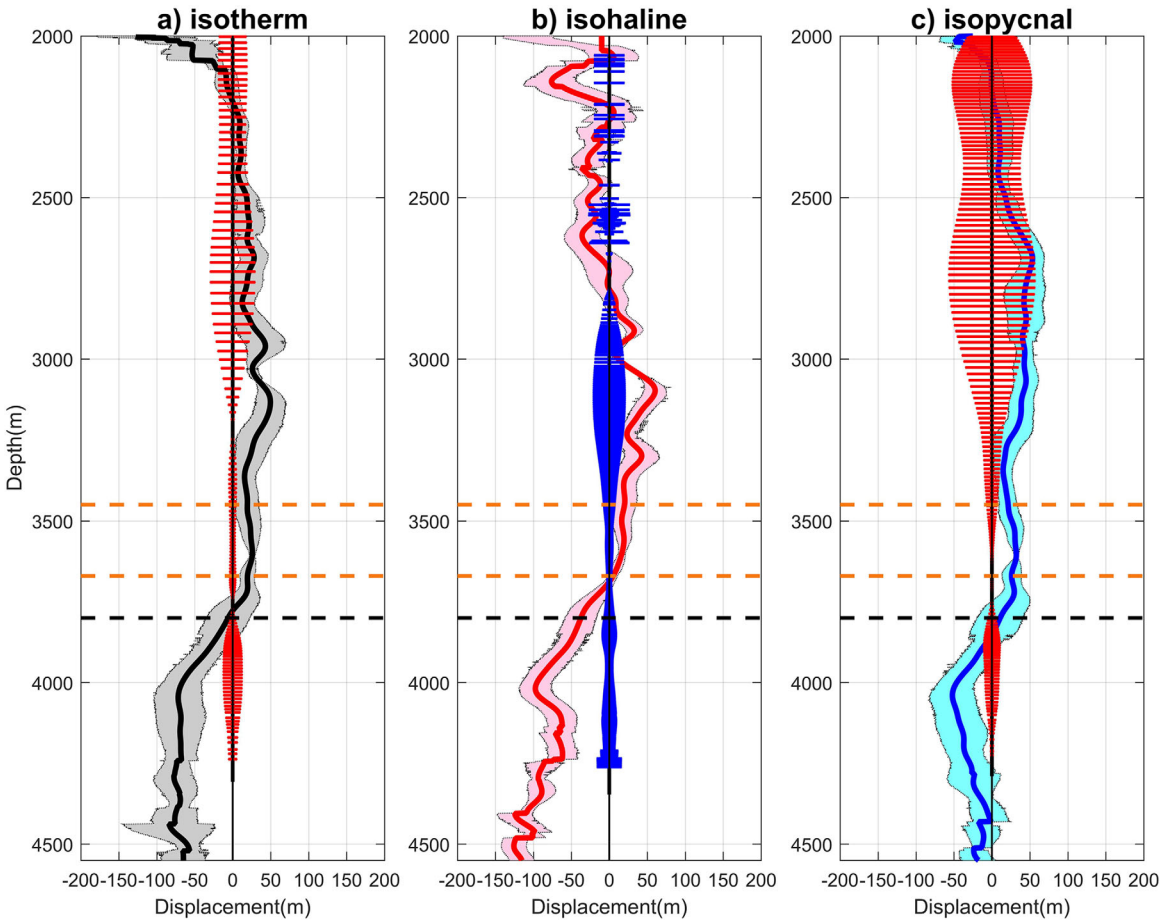

Figure 5. Similar to Figure 4, but showing the difference of the depths of the (a) isotherms, (b) isohalines, and (c) isopycnals between 1997 and 2014. The depth differences and the corresponding uncertainties are calculated in the temperature, salinity, and density coordinate grids. Positive displacements denote upward movement.

was lighter by 0.005 $\pm$ 0.002 kg m^{-3}. The AABW above the canyon is mostly confined to the region west of 16°W and does not show consistent changes across different station pairs (Figure 3). The hydrographic differences in the NADW layer have complicated spatial structures. The 2014 data show cooler and fresher signals in the NADW below 2,500 m over most stations except for the two closest to the sill (Figure 3). Above 2,500 m there is even less spatial coherence in the hydrographic differences. Consequently, the along-canyon averaged changes of temperature, salinity and density (σ_4) in the NADW layer are weak and only statistically significant at limited depth levels below 2,500 m (Figure 4). The most significant change is observed in density near 3,000 m where the NADW was approximately 0.003$\pm$ 0.002 kg m^{-3} denser in 2014 than in 1997.

The hydrographic changes discussed here exceed the short-term variability estimated from the HRP observations collected within 2 weeks (Figure 4). In addition, mesoscale variability can be accounted for by considering the zonal decorrelation length scales of the hydrographic changes. The decorrelation scales are inferred from twice the maximum of the integral of lagged auto-covariance in longitude for both 1997 and 2014. They vary between 80 and 240 km in the water below 2,000 m, which is much smaller than the zonal scale of the hydrographic changes detected here (Figure 3). Therefore, the signals near the canyon very likely reflect the large-scale changes in the Brazil Basin.

We now assess the vertical movement of the isopycnals, isotherms, and isohalines between 1997 and 2014 (Figure 5). Among the 12 station-pairs, the vertical displacements based on the three isopleths display consistent signals below the lateral canyon walls. Within the canyon, the vertical displacement of the AABW isopleths is downward, which is consistent with warmer, saltier, and lighter signals observed at fixed depth levels (Figure 4). The net downward movement of the isotherms and isohalines was about 80 $\pm$ 20 m, but

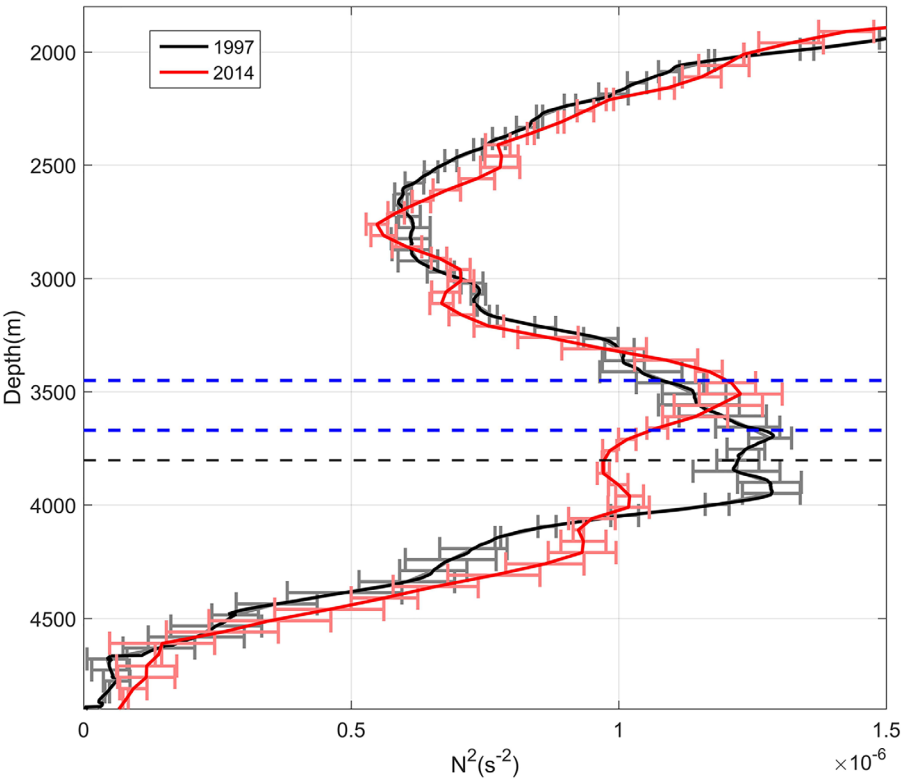

Figure 6. Average profiles of squared buoyancy frequency (N^2) derived from the hydrographic repeat-station profiles collected in 1997(black) and in 2014 (red). The horizontal bars show the 95% confidential limit using a bootstrap method. The blue lines denote the AABW-NADW interface (1.8°C and 2°C isotherms in 2014) and the black line marks the nominal depth of the lateral canyon walls.

the isopycnal displacement had a smaller amplitude (50 ± 20 m), implying partial compensation between the temperature and salinity trends. The isopycnals, isotherms, and isohalines in the NADW layer show mostly positive (i.e., upward) displacements from 1997 to 2014, but these changes at most depth levels are indistinguishable from zero at 95% confidence. Above 3,000 m the temporal variability due to short-term processes has higher magnitude than the changes documented here, implying that caution must be taken in the interpretation of the NADW layer variability.

In order to evaluate the effects of the temperature and salinity changes on the local density stratification, the buoyancy frequency squared, N^2, is calculated for the CTD profile-pairs along the canyon axis (Figure 6). Below 2,000 m, N^2 in 2014 decreased with depth and attained a local minimum around 2,700 m, which coincides with the relatively homogenous NADW core. Below the NADW minimum, the stratification increases downward and reaches a local maximum around 3,500 m near the (nominal) AABW-NADW interface. Within the AABW, N^2 again decreases with depth, with values approaching zero near the bottom. The overall vertical structure of N^2 was not significantly different in 1997 and 2014, except near the NADW-AABW boundary where the local maximum in stratification was thicker and deeper in 1997 compared to 2014. The most significant difference in density stratification between 1997 and 2014 occurs near the peaks of the lateral canyon walls where N^2 in 2014 was about 20% lower than in 1997. The reduced stratification is related to the vertical divergence of the isopycnals in this layer, resulting in greater distances between neighboring isopycnals in 2014 than in 1997.

3.3. Low-Frequency Trend in Density Stratification Over the MAR Flank in the Brazil Basin

In order to provide a large-scale context for the FZ observations, hydrographic profiles along the A16S section are analyzed. This section spans the entire meridional extent of the Brazil Basin along 25°W (Figure 1). The hydrographic differences and the vertical displacement of isotherms between the three occupations of this section were documented by Purkey and Johnson (2010) and Johnson et al. (2014). They found a long-

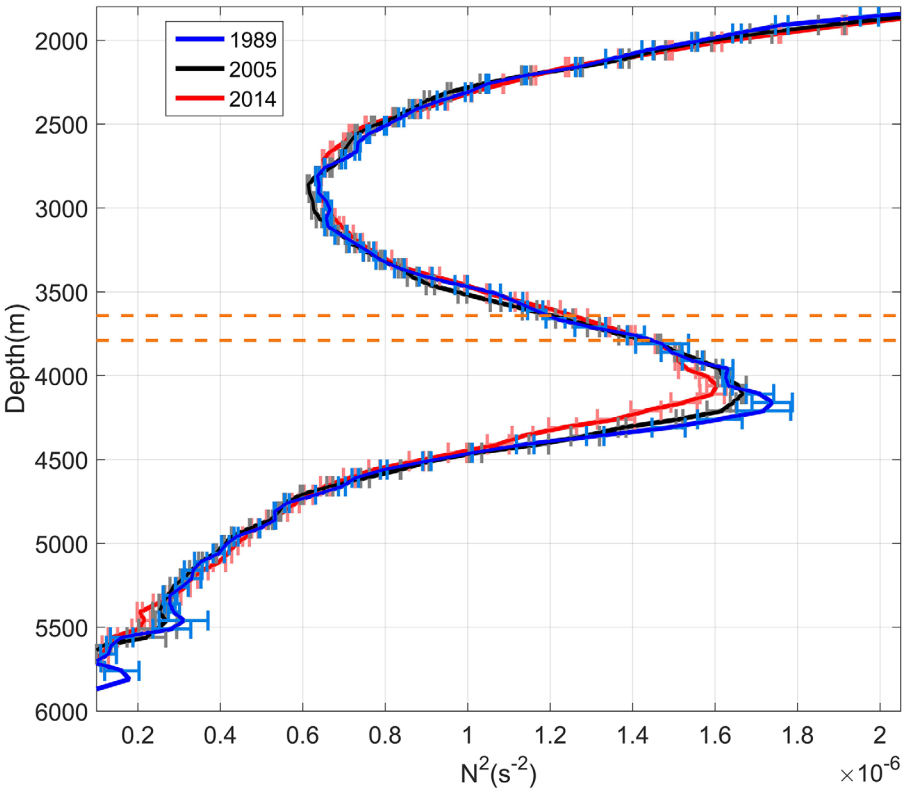

Figure 7. Average profiles of squared buoyancy frequency (N^2) derived from the hydrographic profiles along WOCE A16S section collected in 1989 (blue), 2005 (black), and 2014 (red). The horizontal bars show the 95% confidential limit using a bootstrap method. The orange lines denote the AABW-NADW interface (1.8°C and 2°C isotherms in 2014).

term warming trend and vertical descent of isotherms across the entire abyssal Brazil Basin, consistent with the signals near the canyon presented above. Here we focus on the section-averaged density stratification along 25°W. The resulting profiles of N^2 show similar shapes as those from the FZ canyon. At 25°W, the local minimum in stratification near the NADW core is located near 3,000 m and the local maximum around the NADW-AABW interface is below 4,000 m (Figure 7). These depth levels are deeper than that further east in the FZ canyon. The 1.8°C–2°C isotherms are shallower than the local maximum of N^2, in both the averaged profiles from 25°W and from the canyon near 21°S. The maximum N^2 is higher at 25°W (1.7×10^{-6} s^{-2}) than in the FZ canyon (1.3×10^{-6} s^{-2}). Thus, the density within the AABW layer is less stratified in the canyon than outside, consistent with the higher levels of diapycnal mixing observed there (Thurnherr & Speer, 2003).

The overall structure of the section-averaged N^2 along 25°W was similar in 1989, 2005, and 2014. The most notable changes are observed near the local maximum of N^2 below 4,000 m. From 1989 to 2014, the N^2 is reduced by about 10% and the reduction is significant at the 95% confidence level. This reduction is persistent from 1989 to 2005 and 2005 to 2014, suggesting that it is a multidecadal change. This long-term weakening trend of N^2 over the MAR flank across the full meridional extent of the Brazil Basin is in agreement with the observations from the FZ canyon near 21°S This suggests that the changes observed near the canyon reflect primarily the basinwide changes in the Brazil Basin.

4. Discussion and Conclusions

The hydrographic changes between 1997 and 2014 in and above a FZ canyon in the eastern Brazil Basin near 21°S are documented using repeat-station CTD profiles. The most significant changes are found in the AABW layer, which warmed by 0.08 ± 0.05°C from 1997 to 2014, corresponding to a linear warming rate of 5 ± 3 m °C yr^{-1}. This rate is not significantly different from that found for the overall abyssal Brazil Basin between 1989 and 2014 (2–3 m °C yr^{-1}; Johnson et al., 2014). Furthermore, our inferred warming rate is also consistent with the long-term continuous warming trend of 3 m °C yr^{-1} found in the coldest, densest

waters flowing north into the Brazil Basin through the Vema Channel between 1992 and 2010 (Zenk & Morozov, 2007; Zenk & Visbeck, 2013). A salinification signal of 0.01 ± 0.005 is detected in the AABW layer, and this signal is significantly above the measurement uncertainty of ±0.002. In contrast, no significant salinification was found for the large-scale water mass in the Brazil Basin (Herrford et al., 2017; Johnson et al., 2014). The stable temperature (θ)-salinity relationship implies that salinity is covarying with temperature. A density decrease of 0.005 ± 0.004 kg m^{-3} indicates that temperature dominates the low-frequency density variability.

In contrast to the AABW, the hydrographic changes between 1997 and 2014 in the NADW are much weaker and the weak signals of cooling and densification are only indistinguishable from zero at few depth levels. Similarly, no statistically significant changes in NADW properties were found over three occupations (1989, 1995, and 2014) of A16S in the South Atlantic (Johnson et al., 2014).

The isopycnals, isotherms, and isohalines moved downward in the AABW by 80 ± 20 m between 1997 and 2014. The vertical motion of the isopleths is consistent with the warming and lightening signals analyzed in depth space. The tidal heaving near the canyon is approximately 20–50 m (L. C. St. Laurent et al., 2001). Vertical displacements of 50–100 m on seasonal and interannual time scales were observed for the isotherms within the canyon at 17.8°W (Toole, 2007). Lacking information on the spatial structure for this seasonal and interannual variability, it is hard to diagnose the underlying physical processes for those changes. The bottom water changes found in this study are coherent along the canyon over more than 400 km, which is much greater than the advective length scale associated with the low-frequency along-canyon flow on a yearly time scale (Toole, 2007). Therefore, our results are unlikely contaminated by mesoscale processes but rather reflect the large-scale warming and contraction of the AABW in the Brazil Basin (Purkey & Johnson, 2012). If the displacements between 1997 and 2014 are assumed to be temporally uniform, the mean isothermal fall rate was about 5–6 m/yr. This agrees approximately with the maximum mean isotherm fall rate of 9 m/yr near the 0.3°C isotherm in the Brazil Basin between 1989 and 2005 (Purkey & Johnson, 2012), especially considering that that the isotherm fall rate is larger in the colder (deeper) water.

The vertical structure of the hydrographic changes in the canyon suggest that they are closely tied to the mean along-canyon current and, thus, to the topography. The persistent eastward flow at depth within the canyon provides a direct connection with the deep Brazil Basin, implying that hydrographic changes in the large-scale water masses can easily affect the canyon. For comparison, both Purkey and Johnson (2012) and Johnson et al. (2014) noted that the descent of the isotherms over the entire Brazil Basin becomes negligible around 1.8°C–2°C which coincides with the interface between the AABW and NADW. In contrast, the zero crossings of the temperature and density trends in our analysis correspond better to the crest depths of the lateral sidewalls than to the nominal interface depth between AABW and NADW (Figure 5). The hydrographic changes from 1989 to 2005 and 2005 to 2014 extend from the seabed to far above the local canyon-walls (Johnson et al., 2014). Therefore, the coincidence between the hydrographic changes and the canyon sidewall in our region is likely a local phenomenon. Perhaps, the much weaker zonal velocity above the canyon prevents the zonal spreading of the signals from the deep Brazil Basin at those depths.

The hydrographic changes in and above the canyon also modify the local density stratification. Near its peak, the average squared buoyancy frequency (N^2) shows a statistically significant reduction of up to 20% between 1997 and 2014 near the canyon-wall crests. A similar long-term reduction in N^2 is also found in the averaged stratification profile from the western flank of MAR along 25°W. Qualitatively, such a decrease in density stratification is consistent with the vertical divergence of the mean vertical isopycnal displacements at that depth. Note that the most significant stratification reduction does not correspond to the largest vertical descent of isopycnals, but rather takes place around the local maximum of N^2 and below the isotherms of 1.8°C–2°C. This suggests that the most stratified region in the AABW is more sensitive to the vertical displacement of isopleths.

The observed change the density stratification could well have important implications for the generation and propagation of internal waves. For example, Jayne and St. Laurent (2001) parameterize the internal tide energy extracted from the barotropical tides as

$$E \cong \frac{1}{2}\rho_0 NkU^2h^2 \tag{1}$$

Where ρ_0 is a reference density, N is the buoyancy frequency, k is the horizontal wave number, h is the topographic height, and U is the magnitude of the background barotropic tidal currents. This energy can

feed diapycnal mixing, so that the turbulent diffusivity $k_v \cong \frac{\Gamma q E(x,y) F(z)}{\rho N^2}$ where $\Gamma = 0.2$ represents the mixing efficiency (assumed constant); $q = 0.3 \pm 0.1$ is the fraction of wave energy dissipated locally; *E(x,y)* is the time-averaged internal tide energy flux; $F(z)$ is the vertical structure function of the dissipation and $\int_{-H}^{0} F(z)\, dz = 1$ (Laurent et al., 2002). Using equation (1) for *E(x,y)*, k_v can be rewritten as $\frac{\Gamma q F(z)}{2N} k h^2 U^2$. The wave number k can be inferred from rotary spectra derived from the observed velocity shear near the canyon. The upward energy propagation in the semidiurnal frequency band is dominated by wavelengths between 90 m and about 560 m (Clément et al., 2017). The corresponding horizontal wavelength range inferred from the linear dispersion relationship is 680–4,250 m. Assuming $U = 0.05$ m/s, $h = 200$ m, and taking the mean values at 4,000 m in year 1997 and 2014 for N (i.e., $1.14 \times 10^{-3} s^{-1}$ versus $1.00 \times 10^{-3} s^{-1}$), the parameterized k_v becomes about $3.89–20.26 \times 10^{-4}$ $m^2 s^{-1}$ in 1997 and $4.43–23.1 \times 10^{-4}$ $m^2 s^{-1}$ in 2014. This implies that the observed reduction in N is expected to increase the diffusivity in a 500 m thick layer in the canyon by about 14%. For the A16S section along 25°W, the average maximum buoyancy frequency was 1.32×10^{-3} s^{-1} in 1989 and $1.24 \times 10^{-3} s^{-1}$ in 2014, corresponding to an increase of 6% in the parameterized k_v. According to a heat budget analysis of the Brazil Basin, an increase of vertical diffusivity (k_v) from 4.34×10^{-4} to $4.70 \times 10^{-4} m^2 s^{-1}$, which is about an 8% change, can explain the observed 0.56 Sv volume contraction below 0.8°C (Purkey & Johnson, 2012). Even though our inferred changes in k_v only take place within a deep pycnocline, we expect that they can induce significant volume contraction of the AABW.

Acknowledgments
The DoMORE project was supported by NSF under the grant OCE-1235094. The efforts of colleagues from LDEO, WHOI, and of the officers and crew of the R/V Nathaniel B. Palmer are greatly appreciated. The hydrographic data from the A09 and A16S sections were downloaded from the Clivar & Carbon Hydrographic Data Office (CCHDO) website http://cchdo.ucsd.edu. The BBTRE data used here can be obtained from https://microstructure.ucsd.edu. The DoMore data are available from http://www.marine-geo.org

References

Coles, V. J., McCartney, M. S., Olson, D. B., & Smethie, W. M. (1996). Changes in Antarctic bottom water properties in the western South Atlantic in the late 1980s. *Journal of Geophysical Research*, *101*, 8957–8970. https://doi.org/10.1029/95JC03721

Clément, L., Thurnherr, A. M., & St. Laurent, L. C. (2017). Turbulent mixing in a deep fracture zone on the mid-Atlantic ridge. *Journal of Physical Oceanography*, *47*, 1873–1896. https://doi.org/10.1175/JPO-D-16-0264.1

Desbruyères, D. G., Purkey, S., McDonagh, E. L., Johnson, G. C., & King, B. A. (2016). Deep and abyssal ocean warming from 35 years of repeat hydrography. *Geophysical Research Letters*, *43*, 10,356–10,365. https://doi.org/10.1002/2016GL070413

Hastie, T., Tibshirani, R., & Friedman, J. H. (2009). *The elements of statistical learning: Data mining, inference, and predictions, Springer Series in Statistics* (2nd ed.). New York, NY: Springer.

Herrford, J., Brandt, P., & Zenk, W. (2017). Property changes of deep and bottom waters in the Western Tropical Atlantic. *Deep Sea Research Part I: Oceanographic Research Papers*, *124*, 103–125.

Hogg, N., Biscaye, P. E., Gardner, W. D., & Schmitz, W. J., Jr. (1982). On the transport and modification of Antarctic Bottom Water in the Vema Channel. *Journal of Marine Research*, *40*(Suppl), 231–263.

Hogg, N. G., & Owens, W. B. (1999). Direct measurement of the deep circulation within the Brazil Basin. *Deep Sea Research Part II: Topical Studies in Oceanography*, *46*, 335–353.

Hogg, N. G., Siedler, G., & Zenk, W. (1999). Circulation and variability at the southern boundary of the Brazil Basin. *Journal of Physical Oceanography*, *29*, 145–157.

Hogg, N. G., & Thurnherr, A. M. (2005). A zonal pathway for NADW in the South Atlantic. *Journal of Oceanography*, *61*, 493–507.

Jayne, S. R., & St. Laurent, L. C. (2001). Parameterizing tidal dissipation over rough topography. *Geophysical Research Letters*, *28*, 811–814. https://doi.org/10.1029/2000GL012044

Johnson, G. C., & Doney, S. C. (2006). Recent western South Atlantic bottom water warming. *Geophysical Research Letters*, *33*, L14614. https://doi.org/10.1029/2006GL026769

Johnson, G. C., McTaggart, K. E., & Wanninkhof, R. (2014). Antarctic bottom water temperature changes in the western South Atlantic from 1989 to 2014. *Journal of Geophysical Research: Oceans*, *119*, 8567–8577. https://doi.org/10.1002/2014JC010367

Johnson, G. C., Purkey, S. G., & Toole, J. M. (2008). Reduced Antarctic meridional overturning circulation reaches the North Atlantic Ocean. *Geophysical Research Letters*, *35*, L22601. https://doi.org/10.1029/2008GL035619

Kawano, T., Aoyama, M., Joyce, T., Uchida, H., Takatsuki, Y., & Fukasawa, M. (2006). The latest batch-to-batch difference table of standard seawater and its application to the WOCE onetime sections. *Journal of Oceanography*, *62*, 777–792.

Kouketsu, S., Doi, T., Kawano, T., Masuda, S., Sugiura, N., Sasaki, Y., . . . Awaji, T. (2011). Deep ocean heat content changes estimated from observation and reanalysis product and their influence on sea level change. *Journal of Geophysical Research*, *116*, C03012. https://doi.org/10.1029/2010JC006464

Ledwell, J. R., Montgomery, E. T., Polzin, K. L., St. Laurent, L. C., Schmitt, R. W., & Toole, J. M. (2000). Evidence for enhanced mixing over rough topography in the abyssal ocean. *Nature*, *403*(6766), 179–182. https://doi.org/10.1038/35003164

Munk, W. (1966). Abyssal recipes. *Deep Sea Research and Oceanographic Abstracts*, *13*, 707–730.

Nikurashin, M., & Legg, S. (2011). A mechanism for local dissipation of internal tides generated at rough topography. *Journal of Physical Oceanography*, *41*, 378–395.

Polzin, K. L., Toole, J. M., Ledwell, J. R., & Smith, R. W. (1997). Spatial variability of turbulent mixing in the abyssal ocean. *Science*, *276*, 93–96.

Purkey, S. G., & Johnson, G. C. (2010). Warming of global abyssal and deep Southern Ocean waters between the 1990s and 2000s: Contributions to global heat and sea level rise budgets. *Journal of Climate*, *23*, 6336–6351. https://doi.org/10.1175/2010jcli3682.1

Purkey, S. G., & Johnson, G. C. (2012). Global contraction of Antarctic bottom water between the 1980s and 2000s. *Journal of Climate*, *25*, 5830–5844. https://doi.org/10.1175/jcli-d-11-00612.1

Speer, K. G., Siedler, G., & Talley, L. (1995). The Namib Col Current. *Deep Sea Research Part I: Oceanographic Research Papers*, *42*, 1933–1950.

Speer, K. G., & Zenk, W. (1993). The flow of Antarctic Bottom Water into the Brazil Basin. *Journal of Physical Oceanography*, *23*, 2667–2682.

St. Laurent, L. C., Simmons, H. L., & Jayne, S. R. (2002). Estimating tidally driven mixing in the deep ocean. *Geophysical Research Letters*, *29*(23), 2106. https://doi.org/10.1029/2002GL015633

St. Laurent, L., Toole, J. M., & Schmitt, R. W. (2001). Mixing and diapycnal advection in the ocean. In *Proceedings of the 'Aha Huliko'a Hawaiian Winter Workshop* (pp. 175–185). Honolulu: University of Hawaii.

St. Laurent, L. C., Toole, J. M., & Schmitt, R. W. (2001). Buoyancy forcing by turbulence above rough topography in the abyssal Brazil Basin. *Journal of Physical Oceanography*, *31*, 3476–3495.

Talley, L. D., & Johnson, G. C. (1994). Deep, zonal subequatorial flows. *Science*, *263*, 1125–1128.

Thurnherr, A. M., & Speer, K. G. (2003). Boundary mixing and topographic blocking on the Mid-Atlantic Ridge in the South Atlantic. *Journal of Physical Oceanography*, *33*, 848–862.

Thurnherr, A. M., & Speer, K. G. (2004). Representativeness of meridional hydrographic sections in the Western South Atlantic. *Journal of Marine Research*, *62*, 37–65.

Thurnherr, A. M., St. Laurent, L. C., Speer, K. G., Toole, J. M., & Ledwell, J. R. (2005). Mixing associated with sills in a canyon on the mid-ocean ridge flank. *Journal of Physical Oceanography*, *35*, 1370–1381.

Toole, J. M. (2007). Temporal characteristics of abyssal finescale motions above rough bathymetry. *Journal of Physical Oceanography*, *37*, 409–427.

Whitehead, J. A., & Worthington, L. V. (1982). The flux and mixing rates of Antarctic Bottom Water within the North Atlantic. *Journal of Geophysical Research*, *87*, 7903–7924.

Wilks, D. S. (1997). Resampling hypothesis tests for autocorrelated fields. *Journal of Climate*, *10*, 65–82.

Zenk, W., & Hogg, N. (1996). Warming trend in Antarctic bottom water flowing into the Brazil Basin. *Deep Sea Research Part I: Oceanographic Research Papers*, *43*, 1461–1473.

Zenk, W., Siedler, G., Lenz, B., & Hogg, N. G. (1999). Antarctic bottom water flow through the Hunter Channel. *Journal of Physical Oceanography*, *29*, 2785–2801.

Zenk, W., & Morozov, E. (2007). Decadal warming of the coldest Antarctic Bottom Water flow through the Vema Channel. *Geophysical Research Letters*, *34*, L14607. https://doi.org/10.1029/2007GL030340

Zenk, W., & Visbeck, M. (2013). Structure and evolution of the abyssal jet in the Vema Channel of the South Atlantic. *Deep Sea Research Part II: Topical Studies in Oceanography*, *85*, 244–260. https://doi.org/10.1016/j.dsr2.2012.07.033